World Scientific Research Journal Volume 8 Issue 5, 2022
ISSN: 2472-3703 DOI: 10.6911/WSRJ.202205_8(5).0042

# Automatic Berthing Control of Ships Based on ESO

Yunliang Xu, Diju Gao and Qimeng Xue

Key Laboratory of Transport Industry of Marine Technology and Control Engineering, Shanghai Maritime University, Shanghai, 201306, China

## Abstract

**To address the accuracy reduction of ship's automatic berthing control generated by external disturbance, model uncertainty conditions and inaccurate measurement of velocity, a fast terminal sliding mode is proposed based on extended state observer (ESO) and dynamic surface (DSC). An extended state observer is firstly designed to estimate both velocity and complex perturbations. A dynamic surface control method based on fast terminal sliding mode (FTSM) is proposed. Then, in order to eliminate the computational complexity based on the back-stepping method, the finite time command filter and error compensation signal are adopted in the design of the dynamic surface controller to ensure that the ship reaches the desired berthing position and orientation of the ship. The finite time extended state observer stability of the closed loop system is demonstrated by Lyapunov theory. Finally, the simulation demonstrates the effectiveness of the proposed berthing control method.**

## Keywords

**Automatic berthing; Fast terminal sliding mode (FTSM); Extended state observer (ESO); Dynamic surface (DSC); Model uncertainty.**

## 1. INTRODUCTION

In the process of berthing, the complex traffic environment, unknown external disturbance and model uncertainty caused by wind, waves and flow increase the difficulty of automatic berthing control, which leads to the reduction of control accuracy, making the ship deviate from the berthing trajectory, and even encounter collision accidents. Therefore, this paper further studies external perturbations, model uncertainties and inaccurate velocity measurements, which is of great significance to its application in the field of ship automatic berthing control.

In the study of iterative sliding mode, dynamic output feedback control and neural network control. Literature [1] uses iterative slide mode to design the ship calm controller. Since the initial value of the parameter affects the mixed particle algorithm to modify the initial parameters according to the calculated berthing trajectory deviation, but the computational complexity has increased. Literature [2] proposes the automatic berthing problem of under-actuated surface ships with incomplete acceleration constraints, transforms the trajectory design and tracking problem of the control system into the stabilization control of the scalar zero-order system, and designs the dynamic output feedback controller, but this method is only suitable for front-driving ships. Literature [3] proposes an online trained, back-propagating neural network controller with online adjusted parameters and simulation studies in wind interference and shallow water environments to demonstrate the effectiveness of the proposed method. Literature [4] uses the ESO (ESO, extended state observer) in the self-resistant disturbance controller to estimate the external disturbance information to design the automatic berthing control under the wind and no wind conditions.

ISSN: 2472-3703 DOI: 10.6911/WSRJ.202205_8(5).0042

In the above study, the disturbance is simple to consider in the berthing task, including most of the external wind disturbance, and ignoring the influence of model uncertainty on the berthing control. However, the actual berthing environment is complex and changeable. To this end, literature [5] designs an adaptive neural network controller to estimate external perturbations caused by wind and waves and model uncertainty to enhance the anti-interference of the system and track berthing paths. Literature [6] uses a robust neural network adaptive algorithm to estimate external perturbations and model uncertainty online and designs a back-stepping controller to ensure that the ship reaches the desired berthing position. These use neural network algorithms to estimate external perturbations and model uncertainty are accurate, but the large increase in computational complexity is a problem that cannot be ignored.

In addition, the above study of complex perturbations, model uncertainty design berthing controller is usually asymptotic convergence, which means that in finite time, in contrast, finite time controller can make the system error in finite time, so as to obtain faster convergence rate and better interference suppression characteristics. Literature [7] using finite time perturbation observer estimation model uncertainty and external disturbance, and then based on the global fast non-singular terminal sliding mode to ship finite time berthing, but also based on the ship position and speed state information can be fully measured output feedback control, and considering the external interference, model uncertainty and speed state information measurement inaccurate finite time berthing controller research is less, worth further study.

Under the case of external disturbance, model uncertainty and inaccurate velocity state information measurement, ESO to estimate the speed and complex disturbance, use limited time instruction filter to solve the differential explosion caused by frequent guidance of virtual control law, and introduce the signal generated by error compensation to design the terminal sliding surface to realize rapid convergence. The Lyapunov function is used to prove that the signals of all closed-loop systems can guarantee a bounded closed-loop system stability in a finite time, and finally, the effectiveness of the designed control method is verified through simulation experiments.

## 2. PROBLEM DESCRIPTION

### 2.1. Mathematical Model of Ship Motion

In the process of ship berthing, considering the plane motion in the direction of forward, horizontal drift and bow movement, the model of ship berthing [8] can be expressed as follows.

$$\begin{aligned} &\dot{\boldsymbol{\eta}} = \boldsymbol{R}(\psi)\boldsymbol{v} \\ &\boldsymbol{M}\dot{\boldsymbol{v}} + \boldsymbol{D}\boldsymbol{v} + \boldsymbol{C}(\boldsymbol{v})\boldsymbol{v} + \Delta\boldsymbol{C}\boldsymbol{v} + \Delta\boldsymbol{D}\boldsymbol{v} = \boldsymbol{\tau} + \boldsymbol{d} \end{aligned} \tag{1}$$

Where $\boldsymbol{\eta} = [x, y, \psi]^{\mathrm{T}}$ is the position vector in the earth-fixed frame, consisting of the surge position $x$, the sway position $y$, and the yaw angle $\psi$ of the ship. $\boldsymbol{v} = [u, v, r]^{\mathrm{T}}$ is the velocity vector in the body-fixed frame, consisting of the surge velocity $u$, the sway velocity $v$, the yaw rate $r$ of the ship. $\boldsymbol{M}$ denotes inertia matrix and is positive defining. $\boldsymbol{D}$ is hydrodynamic damping matrix including linear terms and nonlinear terms. $\boldsymbol{C}$ denotes Coriolis matrix. $\boldsymbol{d} = [d_1, d_2, d_3]^{\mathrm{T}}$ denotes disturbance vector, consisting of force $d_1$ in surge, force $d_2$ in sway and moment $d_3$ in yaw. $\boldsymbol{\tau} = [\tau_1, \tau_2, \tau_3]^{\mathrm{T}}$ control forces or moments, consisting of force $\tau_1$ in surge, force $\tau_2$ in sway and moment $\tau_3$ in yaw. denotes model uncertainty; $\boldsymbol{U}_d = \boldsymbol{d} - \boldsymbol{\Delta}_f$

ISSN: 2472-3703 DOI: 10.6911/WSRJ.202205_8(5).0042

denotes complex perturbation vectors consisting of the model uncertainty and external perturbations; $\boldsymbol{\eta}_d = [x_d, y_d, \psi_d]^{\mathrm{T}}$ denotes desired point, $\boldsymbol{R}(\psi)$ is the rotation matrix given by:

$$\boldsymbol{R}(\psi) = \begin{bmatrix} \cos\psi & -\sin\psi & 0 \\ \sin\psi & \cos\psi & 0 \\ 0 & 0 & 1 \end{bmatrix} \tag{2}$$

Assumption 1: The external disturbance of the ship during the berthing process is bounded and there exists $\varepsilon_d$ the norm bound of the external disturbance derivatives such that

$$\left\| \dot{\boldsymbol{d}}(\mathrm{t}) \right\| \le \varepsilon_d < \infty \tag{3}$$

Assumption 2: The model uncertainty of the ship is unknown and bounded and there exists the norm bound of the model uncertainty derivatives such that

$$\left\| \dot{\boldsymbol{d}}(\mathrm{t}) - \dot{\Delta}_f(\mathrm{t}) \right\| \le \varepsilon_d + \varepsilon_{\Delta f} \le U_d^* \tag{4}$$

According to assumption 1and assumption 2， complex perturbations can be obtained, where the norm bounds of the complex perturbation derivatives

Assumption 3: The velocity vector of the ship cannot be measured [9].

Define two new auxiliary variables $x_1 = \boldsymbol{\eta}$ , $x_2 = \dot{\boldsymbol{\eta}}$ the equation(1) can be rewritten as follows.

$$\begin{aligned} \dot{x}_1 &= x_2 \\ \dot{x}_2 &= J(\psi)\boldsymbol{M}^{-1}(\boldsymbol{D}(\boldsymbol{v})\boldsymbol{v} + \boldsymbol{C}(\boldsymbol{v})\boldsymbol{v} + \boldsymbol{U}_{\mathrm{d}}) + \dot{J}(\psi)\boldsymbol{v} + J(\psi)\boldsymbol{M}^{-1}\boldsymbol{\tau} \end{aligned} \tag{5}$$

## 3. CONTROL SYSTEM DESIGN

### 3.1. Control Objection

The control goal of this paper is to target the mathematical model of fully drive ship, considering the case of ship model uncertainty, external disturbance and inaccurate speed measurement, and the assumption is established. Based on the finite time DSC method of ESO and FTSM, the problem of automatic berthing stabilization control with external interference, uncertain parameters and immeasurable velocity of ships are solved. A fixed time ESO is proposed to estimate external interference, model uncertainty and ship speed, and then design the ship automatic berthing controller based on improved DSC method of FTSM to make the ship reach the desired berthing position, so as to complete the automatic berthing task. The block diagram of the control system is shown in Figure 1.

ISSN: 2472-3703 DOI: 10.6911/WSRJ.202205_8(5).0042

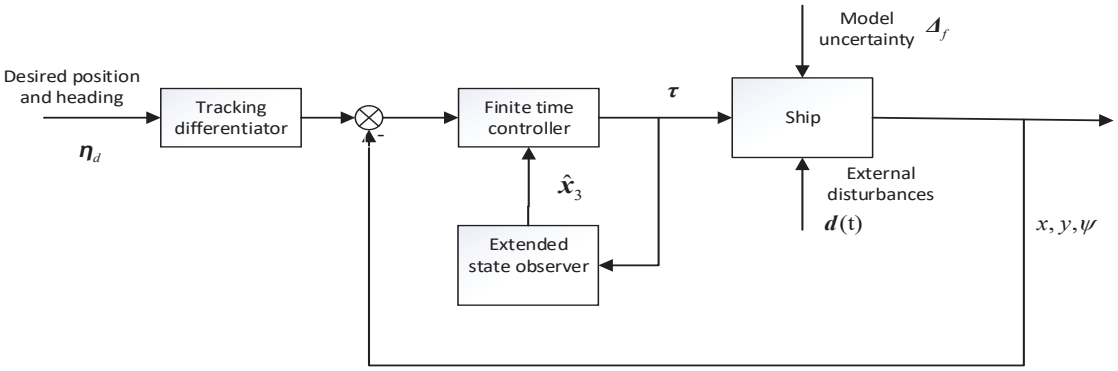


**Figure 1.** Block diagram of the control system

### 3.2. Fixed-time Extended State Observer Design

Define the $\hat{x}_1, \hat{x}_2, \hat{x}_3$ estimation of $x_1, x_2, x_3$ and the estimation error as $e_1 = \hat{x}_1 - x_1$, $e_2 = \hat{x}_2 - x_2$ and $\tilde{x}_3 = \hat{x}_3 - x_3$ respectively, then design the following fixed time extended state observer.

$$\begin{cases} \dot{\hat{x}}_1 = -\kappa_1 \left[ |e_1|^{\alpha_1} \operatorname{sign}(e_1) - |e_1|^{\beta_1} \operatorname{sign}(e_1) \right] + \hat{x}_2 \\ \dot{\hat{x}}_2 = -\kappa_2 \left[ |e_1|^{2\alpha_1 - 1} \operatorname{sign}(e_1) - |e_1|^{2\beta_1 - 1} \operatorname{sign}(e_1) \right] - J(\psi) M^{-1} \boldsymbol{\tau} + \hat{x}_3 \\ \dot{\hat{x}}_3 = -\kappa_3 \left[ |e_1|^{3\alpha_1 - 2} \operatorname{sign}(e_1) - |e_1|^{3\beta_1 - 2} \operatorname{sign}(e_1) \right] \end{cases} \tag{6}$$

Where $2/3 < \alpha_1 < 1$, $\beta_1 > 1, \kappa_i (i = 1, 2, 3)$ is positive and satisfies $\kappa_3 < \kappa_1 \kappa_2$. According to the equation(5) and (6), the dynamic observation error can be obtained as follows.

$$\begin{cases} \dot{e}_1 = -\kappa_1 \left[ |e_1|^{\alpha_1} \operatorname{sign}(e_1) - |e_1|^{\beta_1} \operatorname{sign}(e_1) \right] + e_2 \\ \dot{e}_2 = -\kappa_2 \left[ |e_1|^{2\alpha_1 - 1} \operatorname{sign}(e_1) - |e_1|^{2\beta_1 - 1} \operatorname{sign}(e_1) \right] + e_3 \\ \dot{e}_3 = -\kappa_3 \left[ |e_1|^{3\alpha_1 - 2} \operatorname{sign}(e_1) - |e_1|^{3\beta_1 - 2} \operatorname{sign}(e_1) \right] - g_1(t) \end{cases} \tag{7}$$

The following proof considers a ship model in the presence of external disturbances and model uncertainty. If this exists, and the fixed time ESO is expressed in the form Eq. (6), then there is a region in which the error dynamic system is globally fixed time convergent.

Step 1: First define the nominal system for the dynamic observation error Eq. (7) as:

$$\dot{\boldsymbol{e}} = F_\alpha(\boldsymbol{e}) \tag{8}$$

where $F_\alpha(\boldsymbol{e})$ denotes a continuous vector field and is defined as:

$$F_\alpha(\boldsymbol{e}) = \begin{bmatrix} e_2 - \kappa_1 |e_1|^{\alpha_1} \operatorname{sign}(e_1) \\ e_3 - \kappa_2 |e_1|^{2\alpha_1 - 1} \operatorname{sign}(e_1) \\ -\kappa_3 |e_1|^{3\alpha_1 - 2} \operatorname{sign}(e_1) \end{bmatrix} \tag{9}$$

ISSN: 2472-3703 DOI: 10.6911/WSRJ.202205_8(5).0042

It can be verified that the vector field $F_\alpha(\boldsymbol{e})$ is homogeneous of degree with $\alpha-1<0$ to the weight vectors $r_\alpha=\{(i-1)\alpha-(i-2),i=1,2,3\}$ and, in addition, the system matrix $A$ is defined to be the Hurwitz matrix.

$$A=\begin{bmatrix}-\kappa_1 I_3 & I_3 & 0\\ -\kappa_2 I_3 & 0 & I_3\\ -\kappa_3 I_3 & 0 & 0\end{bmatrix} \tag{10}$$

Then, the Lyapunov function is constructed for the observation error system Eq. (8) as follows.

$$V_\alpha\left(e_1,e_2,e_3\right)=\frac{1}{2}\zeta^T P\zeta \tag{11}$$

Where $\zeta=\left[\left[\mathrm{sig}^{1/\omega}\left(e_1\right)\right]^T,\left[\mathrm{sig}^{1/\omega\alpha_1}\left(e_2\right)\right]^T,\left[\mathrm{sig}^{1i\omega\alpha_2}\left(e_3\right)\right]^T\right]^T,\omega=\alpha_1\alpha_2\alpha_3,\quad P\in R^{9\times 9}$ is the solution of the equation $A^TP+PA=-I_9$. $V_\alpha\left(e_1,e_2,e_3\right)$ is the Lyapunov function of the system (8). It can be verified that the vector $V_\alpha\left(e_1,e_2,e_3\right)$ is homogeneous of degree with $d_1=\frac{2}{\omega}$ to the weight vectors $r_\alpha$.

Let $L_FV_\alpha\left(e_1,e_2,e_3\right)$ denote the Lie derivative $V_\alpha$ along the vector field $F_\alpha(x)$ and one obtains $L_FV_\alpha\left(e_1,e_2,e_3\right)$ that the vector $L_FV_\alpha\left(e_1,e_2,e_3\right)$ has homogeneous of degree with $d_2=\frac{2}{\omega}+\alpha-1$ to the weights vectors $r_\alpha$.Therefore, it follows from Lemma 4.2 in literature [10] that there are positive parameters $\mu_1=-\max_{\{eV_\alpha(e)=1\}}L_FV_\alpha\left(e_1,e_2,e_3\right)$ such that the following inequality holds:

$$L_FV_\alpha\left(e_1,e_2,e_3\right)\le-\mu_1V_\alpha^{d_m} \tag{12}$$

Where $d_m=\frac{d_2}{d_1}=1+\frac{\omega(\alpha-1)}{2}<1$ .

Next, the following dynamic system is considered separately, the observation error dynamics Eq. (7) is designed as:

$$\dot{\boldsymbol{e}}=F_\beta(e) \tag{13}$$

Where $F_\beta(e)$ denotes the continuous vector field can be expressed as:

$$F_\beta(e)=\begin{bmatrix}-\kappa_1\left|e_1\right|^{\beta_1}\mathrm{sign}\left(e_1\right)\\ -\kappa_2\left|e_1\right|^{2\beta_1-1}\mathrm{sign}\left(e_1\right)\\ -\kappa_3\left|e_1\right|^{3\beta_1-2}\mathrm{sign}\left(e_1\right)\end{bmatrix} \tag{14}$$

ISSN: 2472-3703 DOI: 10.6911/WSRJ.202205_8(5).0042

It is easy to verify that the vector field $F_\beta(e)$ is homogeneous of degree with $\beta-1>0$ to the weight vector $r_\beta$. Construct the Lyapunov function for the dynamical system Eq. (13) as follows:

$$V_\beta(e_1,e_2,e_3)=\frac{1}{2}\zeta^T P\zeta \tag{15}$$

Where the definitions of $\zeta$ and $P$ are the same as in equation (11).

It can be obtained that the vector $V_\beta(e_1,e_2,e_3)$ is homogeneous of degree with $d_3=\frac{2}{\omega}$ to the weight vector $r_\alpha$. $L_F V_\beta(e_1,e_2,e_3)$ denote the Lie derivative of $V_\beta(e_1,e_2,e_3)$ along the vector field $F_\beta(e)$, and $L_F V_\beta(e_1,e_2,e_3)$ is homogeneous of degree with $d_4=\frac{2}{\omega}+\beta-1$ to the weights vectors $r_\alpha$ . Therefore, it follows from Lemma 4.2 in literature [10]that there are positive parameters $\mu_2=-\max_{\{eV_\beta(e)=1\}} L_F V_\beta(e_1,e_2,e_3)$ such that the following inequality holds:

$$L_F V_\beta(e_1,e_2,e_3)\le-\mu_2 V_\beta^{d_n} \tag{16}$$

Where, $d_m=\frac{d_2}{d_1}=1+\frac{\omega(\beta-1)}{2}>1$ .

Based on the above analysis of Eq. (8) and (13), the following Lyapunov function is constructed for the complete double power fixed time dilation state observer Eq. (6):

$$V_0(e_1,e_2,e_3)=\frac{1}{2}\zeta^T P\zeta \tag{17}$$

Where the definitions of $\zeta$ and $P$ are the same as in Eq. (11).

Taking the time derivative of Eq. (17) along Eq. (7) yields:

$$\dot{V}_0(e_1,e_2,e_3)=L_F V_\alpha(e_1,e_2,e_3)+L_F V_\beta(e_1,e_2,e_3)+\sum_{i=1}^{3}\frac{\partial V_\beta(e_1,e_2,e_3)}{\partial e_{3,i}}\phi_i(t) \tag{18}$$

Since $V_\beta(e_1,e_2,e_3)$ is homogeneous of degree with $d_3=\frac{2}{\omega}$ to the weight vector $r_\alpha$ .It follows from Lemma 5.1in literature [11] that the vector $\frac{\partial V_\beta(e_1,e_2,e_3)}{\partial e_{3,i}}$ is homogeneous of degree with $d_5=1+\frac{2}{\omega}-2\alpha>0$ to the weight vector $r_\alpha$ . There exist real numbers $\mu_{3,i}=\min_{\{eV_\beta(e)=1\}}\frac{\partial V_\beta(e_1,e_2,e_3)}{\partial e_{3,i}}$ and $\mu_{4,i}=\max_{\{e:V_\beta(e)=1\}}\frac{\partial V_\beta(e_1,e_2,e_3)}{\partial e_{3,i}}$ such that the following inequality holds:

ISSN: 2472-3703 DOI: 10.6911/WSRJ.202205_8(5).0042

$$\mu_{3,i}V_\beta^{\frac{\omega d_s}{2}} \le \frac{\partial V_\beta\left(e_1,e_2,e_3\right)}{\partial e_{3,i}} \le \mu_{4,i}V_\beta^{\frac{\omega d_s}{2}} \tag{19}$$

Substituting Eq. (12) and Eq. (16) into Eq. (18) yields:

$$\begin{aligned}\dot{V}_0 &\le -\mu_1 V_0^{d_m} - \mu_2 V_0^{d_n} + \sum_{i=1}^{3}\frac{\partial V_\beta\left(e_1,e_2,e_3\right)}{\partial e_{3,i}} g_i(t) \\ &\le -\mu_1 V_0^{d_m} - \mu_2 V_0^{d_n} + \mu_\beta \bar{g} V_0^{\frac{\omega d_3}{2}}\end{aligned} \tag{20}$$

Where $\mu_\beta = \sum_{i=1}^{3}\max\left\{\left|\mu_{3,i}\right|,\left|\mu_{4,i}\right|\right\}$.

According to Lemma 5.3 in literature [11] , $V_0(e)$ the convergence to the following bounded region can be achieved in fixed time $T_1$.

$$V_0(e) < \left(\frac{\mu_\beta \bar{g}}{\mu_2 \varsigma}\right)^{\overline{2d_n-\omega d_5}} \triangleq \bar{V}_0 \tag{21}$$

$V_0(e)$ the convergence time from the initial moment $t_0$ to the final convergence $\bar{V}_0$ in the bounded region is satisfied.

$$t_1 \le T_1 = \frac{1}{\mu_1\left(1-d_m\right)} + \frac{1}{\mu_2(1-\varsigma)\left(d_n-1\right)} \tag{22}$$

So, there is a region with global fixed time convergence when time $t > T_1$ is satisfied and the convergence time $T_1$ does not depend on the initial conditions. Therefore, it is reasonable to conclude that the observation error is bounded, and for the convenience of the subsequent controller design, the upper bound on the observation error is defined as $b_1$.

### 3.3. Design A Finite-time Dynamic Surface Controller

In this subsection, an FTSM-based dynamic surface controller is designed by using an improved virtual control signal and an error compensation signal.

Step 1: Define the position error $e_{z1} = \boldsymbol{J}^{\mathrm{T}}(\boldsymbol{\eta}_1 - \boldsymbol{\eta}_d)$, where $\boldsymbol{\eta}_d$ is the desired berthing position. Design the virtual control law as follows.

$$\beta = -a_1 e_{z1} + \dot{\boldsymbol{\eta}}_d - l_1\left|v_1\right|^{\alpha_2}\operatorname{sign}\left(v_1\right) - \boldsymbol{J}^{\mathrm{T}}(r)e_{z1} \tag{23}$$

Where $a_1$ and $l_1$ are positive definite symmetric matrices, $\alpha_2 \in (0,1)$ . To deal with the problem of "differential explosion" in the inverse step method, the following finite-time filter is designed as follows.

ISSN: 2472-3703 DOI: 10.6911/WSRJ.202205_8(5).0042

$$\begin{cases} \dot{\beta}_f = -r_1 \left| \beta_f - \beta \right|^{\frac{1}{2}} \operatorname{sign}\left( \beta_f - \beta \right) + \varphi_1 \\ \dot{\varphi}_1 = -r_2 \operatorname{sign}\left( \varphi_1 - \dot{\beta}_f \right) \end{cases} \tag{24}$$

Where $r_1$ and $r_2$ are positive definite symmetric matrices, $\beta_f$ is the filtered output of $\beta$ and $\varphi_1$ is the filtered output of $\dot{\beta}_f$. According to Lemma 5 in the literature [12], we can obtain $\left| \beta_f - \beta \right| \le \sigma_1$, where $\sigma_1$ is a positive number and depends on the design parameters of the filter

Define the velocity error $e_{z2} = \boldsymbol{v} - \beta_f$ .In order to reduce the filtering error, the following signal is defined to compensate for the tracking error.

$$\begin{cases} \dot{\xi}_1 = \beta_f - \beta - l_2 \left| \xi_1 \right|^{\gamma_1} \operatorname{sign}\left( \xi_1 \right) - a_1 \xi_1 + \xi_2 \\ \dot{\xi}_2 = -l_3 \left| \xi_2 \right|^{\gamma_1} \operatorname{sign}\left( \xi_2 \right) - a_2 \xi_2 - \xi_1 \end{cases} \tag{25}$$

Where $l_2, l_3$ are positive definite symmetric matrices, $\gamma_1 \in (0,1)$ .

Step 2: A FTSM [13] is designed as follows.

$$s_1 = v_2 + r_3 F\left( v_1 \right) + r_4 \left| v_1 \right|^{\alpha_4} \operatorname{sign}\left( v_1 \right) \tag{26}$$

Where $r_3$ and $r_4$ are positive definite symmetry matrices. The function $F\left( v_1 \right)$ is denoted as follows.

$$F\left( v_1 \right) = \begin{cases} \left| v_1 \right|^{\alpha_3} \operatorname{sign}\left( v_1 \right) & \text{if } \bar{s}_1 = 0 \text{ or } \bar{s}_1 \ne 0, \left| v_1 \right| > c_2 \\ r_5 v_1 + r_6 \left| v_1 \right|^2 \operatorname{sign}\left( v_1 \right) & \text{if } \bar{s}_1 \ne 0, \left| v_1 \right| \le c_2 \end{cases} \tag{27}$$

Where $\bar{s}_1 = v_2 + r_3 \left| v_1 \right|^{\alpha_3} \operatorname{sign}\left( v_1 \right) + r_4 \left| v_1 \right|^{\alpha_4} \operatorname{sign}\left( v_1 \right), 0 < \alpha_3 < 1, \quad \alpha_4 > 1, \quad r_5 = \left( 2 - \alpha_3 \right) c_2^{\alpha_3 - 1}$ is a small positive number. It is worth noting that the above designed sliding surface not only solves the singularity problem but also has a faster convergence rate when $\alpha_4 > 1$ .

The derivative of $F\left( v_1 \right)$ yields:

$$\dot{F}\left( v_1 \right) = \begin{cases} \alpha_3 \left| v_1 \right|^{\alpha_3 - 1} \dot{v}_1 & \text{if } \bar{s}_1 = 0 \text{ or } \bar{s}_1 \ne 0, \left| v_1 \right| \ge c_2 \\ r_5 \dot{v}_1 + 2 r_6 \left| v_1 \right| \dot{v}_1 & \text{if } \quad \bar{s}_1 \ne 0, \left| v_1 \right| \le c_2 \end{cases} \tag{28}$$

Then the finite time controller is designed as follows.

$$\begin{aligned} \boldsymbol{\tau} = \boldsymbol{M} \Big[ & -\boldsymbol{J}^{\mathrm{T}}(\psi) \boldsymbol{R}^{\mathrm{T}}(r) x_2 + \dot{\beta}_f - \boldsymbol{J}^{-1}(\psi) \hat{x}_3 - \hat{b}_1 \operatorname{sign}\left( s_1 \right) - l_3 \left| \xi_2 \right|^{\gamma_1} \operatorname{sign}\left( \xi_2 \right) - a_2 \xi_2 \\ & - r_3 \dot{F}\left( v_1 \right) - r_4 \alpha_4 \left| v_1 \right|^{\alpha_4 - 1} \dot{v}_1 - \varepsilon_1 \left| s_1 \right|^{\alpha_2} \operatorname{sign}\left( s_1 \right) - \varepsilon_2 s_1 - e_{z1} \Big] \end{aligned} \tag{29}$$

ISSN: 2472-3703 DOI: 10.6911/WSRJ.202205_8(5).0042

Where $\hat{b}_1$ is the estimated value of $b_1$ and $\tilde{b}_1$ is the estimated error of $b_1$ and can be updated by the following adaptive law .

$$\dot{\hat{b}}_1 = \lambda_1 |s_1| - \lambda_2 \hat{b}_1 \tag{30}$$

Where, $\lambda_1 > 0, \lambda_2 > 0, \hat{b}_1(0) \geq 0$. According to Lemma 2 in the literature [14], it is possible to obtain $0 < \hat{b}_1 < \bar{b}_1$, where $\bar{b}_1$ is a positive scalar.

### 3.4. Stability Analysis

Select the Lyapunov function as follows.

$$V_1 = \frac{1}{2} v_1^{\mathrm{T}} v_1 + \frac{1}{2} s_1^{\mathrm{T}} s_1 + \frac{1}{2\lambda_1} \tilde{b}_1^{\mathrm{T}} \tilde{b}_1 \tag{31}$$

$$\begin{aligned} \dot{V}_1 &= v_1 \dot{v}_1 + s_1 \dot{s}_1 + \frac{1}{\lambda_1} \tilde{b}_1 \dot{\hat{b}}_1 \\ &= v_1 \left[ \boldsymbol{R}^{\mathrm{T}}(r) e_{z1} + \mathrm{v} - \boldsymbol{J}^{\mathrm{T}}(\psi) \dot{\eta}_d - \dot{\xi}_1 \right] + s_1 \dot{s}_1 + \frac{1}{\lambda_1} \tilde{b}_1 \dot{\hat{b}}_1 + s_1 \dot{s}_1 + \frac{1}{\lambda_1} \tilde{b}_1 \dot{\hat{b}}_1 \\ &= v_1 \left[ v_2 - a_1 v_1 - l_1 |v_1|^{\alpha_2} \operatorname{sign}(v_1) + l_2 |\xi_1|^{\gamma_1} \operatorname{sign}(\xi_1) \right] \end{aligned} \tag{32}$$

The derivative of the slide mode surface can be rewritten as follows.

$$\begin{aligned} \dot{s}_1 &= \dot{v}_2 + r_3 \dot{F}(V_1) + r_4 \alpha_4 |v_1|^{\alpha_4 - 1} \dot{v}_1 \\ &= \dot{e}_{z2} - \dot{\xi}_2 + r_3 \dot{F}(V_1) + r_4 \alpha_4 |v_1|^{\alpha_4 - 1} \dot{v}_1 \\ &= \dot{v} - \dot{\beta}_f - \dot{\xi}_2 + r_3 \dot{F}(V_1) + r_4 \alpha_4 |v_1|^{\alpha_4 - 1} \dot{v}_1 \\ &= \boldsymbol{J}^{\mathrm{T}}(\psi) \boldsymbol{R}(r) x_2 + \boldsymbol{J}^{-1}(\psi) x_3 + M^{-1} \tau - \dot{\beta}_f - \dot{\xi}_2 + r_3 \dot{F}(V_1) + r_4 \alpha_4 |v_1|^{\alpha_4 - 1} \dot{v}_1 \\ &= -\boldsymbol{J}^{-1} \tilde{x}_3 - \hat{b}_1 \operatorname{sign}(s_1) - \varepsilon_1 |s_1|^{\alpha_2} \operatorname{sign}(s_1) - \varepsilon_2 s_1 - v_1 \end{aligned} \tag{33}$$

Taking the adaptive law (30) and formula (33) into formula (32) yields:

$$\begin{aligned} \dot{V}_1 &= \dot{V}_1 + s_1 \left[ -\boldsymbol{J}^{-1} \tilde{x}_3 - \hat{b}_1 \operatorname{sign}(s_1) - \varepsilon_1 |s_1|^{\alpha_2} \operatorname{sign}(s_1) - \varepsilon_2 s_1 - v_1 \right] \\ &\quad + \frac{1}{\lambda_1} \tilde{b}_1 \left( \lambda_1 |s_1| - \lambda_2 \hat{b}_1 \right) \\ &= \dot{V}_1 + s_1 \left[ -\boldsymbol{J}^{-1} \tilde{x}_3 - \hat{b}_1 \operatorname{sign}(s_1) - \varepsilon_1 |s_1|^{\alpha_2} \operatorname{sign}(s_1) - \varepsilon_2 s_1 - v_1 \right] \\ &\quad + \tilde{b}_1 |s_1| - \frac{\lambda_2}{\lambda_1} \tilde{b}_1 \hat{b}_1 \end{aligned} \tag{34}$$

ISSN: 2472-3703 DOI: 10.6911/WSRJ.202205_8(5).0042

$$\begin{aligned}\dot{V}_1 &\le -l_1\left|v_1\right|^{\alpha_2+1}+v_1\left[s_1-r_3F\left(v_1\right)-r_4\left|v_1\right|^{\alpha_4}\operatorname{sign}\left(v_1\right)\right]+\frac{l_2}{2}c_1^{2\gamma_1}\\&\quad+\left|s_1\right|\left\|\tilde{x}_3\right|-\hat{b}_1\left|s_1\right|-\varepsilon_1\left|s_1\right|^{\alpha_2+1}-s_1v_1+\tilde{b}_1\left|s_1\right|-\frac{\lambda_2}{\lambda_1}\tilde{b}_1\hat{b}_1\\&\le -l_1\left|v_1\right|^{\alpha_2+1}-r_3v_1F\left(v_1\right)+\frac{l_2}{2}c_1^{2\gamma_1}-\varepsilon_1\left|s_1\right|^{\alpha_2+1}-\frac{\lambda_2}{\lambda_1}\tilde{b}_1\hat{b}_1\end{aligned}\tag{35}$$

According to Eq. (28) it is obtained as:

$$v_1F\left(v_1\right)=\begin{cases}\left|v_1\right|^{\alpha_3+1} & \text{if } \bar{s}_1=0 \text{ or } \bar{s}_1\ge 0,\left|v_1\right|>c_2\\ r_5v_1^2+r_6\left|v_1\right|^3 & \text{if } \bar{s}_1\ge 0,\left|v_1\right|\le c_2\end{cases}\tag{36}$$

$$\begin{aligned}\dot{V}_1 &\le -l_1\left|v_1\right|^{\alpha_2+1}+\frac{l_2}{2}c_1^{2\gamma_1}-\varepsilon_1\left|s_1\right|^{\alpha_2+1}-\frac{\lambda_2}{\lambda_1}\tilde{b}_1\hat{b}_1\\&=-l_1\left|v_1\right|^{\alpha_2+1}-\varepsilon_1\left|s_1\right|^{\alpha_2+1}-\frac{\lambda_2}{\lambda_1}\left|\tilde{b}_1\right|^{\alpha_2+1}+\frac{\lambda_2}{\lambda_1}\left|\tilde{b}_1\right|^{\alpha_2+1}-\frac{\lambda_2}{\lambda_1}\left(\tilde{b}_1\right)\hat{b}_1+\frac{l_2}{2}c_1^{2\gamma_1}\end{aligned}\tag{37}$$

The equation of (37) $\lambda_2\left(\left|\hat{b}_1-b_1\right|^{\alpha_2+1}-\left(\hat{b}_1-b_1\right)\hat{b}_1\right)/\lambda_1$ satisfied the following inequality when $\hat{b}_1>0$.

$$\frac{\lambda_2}{\lambda_1}\left|\tilde{b}_1\right|^{\alpha_2+1}-\frac{\lambda_2}{\lambda_1}\left(\tilde{b}_1\right)\hat{b}_1=\frac{\lambda_2}{\lambda_1}\left[\left|\tilde{b}_1\right|^{\alpha_2+1}-\left(\tilde{b}_1\right)^2-\tilde{b}_1b_1\right]\tag{38}$$

(1) When $0<\left|\hat{b}_0-b_0\right|<1$, using the basic attributes, the following inequality is constructed as follows.

$$0\le\left|\hat{b}_1-b_1\right|^{\alpha_2+1}-\left|\hat{b}_1-b_1\right|^2\le\zeta_1\tag{39}$$

Where $\zeta_1=c_2^{c_2/(1-c_2)}-c_2^{1/(1-c_2)}$, $c_2=0.5\left(\alpha_2+1\right)$

(2) When $\left|\hat{b}_0-b_0\right|>1$ ,the following inequality is constructed as follows.

$$\left|\hat{b}_1-b_1\right|^{\alpha_2+1}-\left|\hat{b}_1-b_1\right|^2<0\tag{40}$$

Regardless the value of $\left|\hat{b}_0-b_0\right|$,the equation of $\left|\hat{b}_1-b_1\right|^{\alpha_2+1}-\left|\hat{b}_1-b_1\right|^2\le\zeta_1$ is established, so the equation(37)can be rewritten as :

$$\dot{V}_1\le -l_1\left|v_1\right|^{\alpha_2+1}-\varepsilon_1\left|s_1\right|^{\alpha_2+1}-\frac{\lambda_2}{\lambda_1}\left|\hat{b}_1-b_1\right|^{\alpha_2+1}+\frac{\lambda_2}{\lambda_1}\left(\zeta_1+b_1^2\right)+\frac{l_2}{2}c_1^{2\gamma_1}\le -p_1V_2^{\frac{\alpha_2+1}{2}}+c_3\tag{41}$$

ISSN: 2472-3703 DOI: 10.6911/WSRJ.202205_8(5).0042

Where $p_1 = 2^{0.5(\alpha_2+1)} \min\left\{l_1, \varepsilon_1, \lambda_2 \lambda_1^{0.5(\alpha_2-1)}\right\}$, $c_3 = \lambda_2\left(\zeta_1 + b_1^2\right)/\lambda_1 + 0.5 l_2 c_1^{2\gamma_1}$.

Based on the above analysis, it is concluded that the system is actually stable in a finite time.

## 4. SIMULATION STUDIES

During the berthing process of the ship, considering the influence of external disturbances as well as model uncertainties, ignoring its restricted trajectory by the berthing environment and shore wall effects in achieving the automatic berthing task, the parameters of the ship will refer to a supply ship [15] as the simulation object for simulation tests, so the first-order Markov process [16] is used to describe the external disturbances to which the ship is subjected as follows.

$$\begin{cases} \boldsymbol{d} = \boldsymbol{R}^{\mathrm{T}}(\psi)\boldsymbol{b} \\ \dot{\boldsymbol{b}} = -\boldsymbol{T}_{\mathrm{c}}^{-1}\boldsymbol{b} + \boldsymbol{\rho}\boldsymbol{n} \end{cases} \tag{42}$$

Where $\boldsymbol{b}$ is the external disturbance vector ,the disturbance initial value $\boldsymbol{b}(0) = [10^4, 10^4, 10^4]^{\mathrm{T}}$; $\boldsymbol{T}_{\mathrm{c}}(0) = diag\{10^3, 10^3, 10^3\}$ is the designed time-constant diagonal array; $\boldsymbol{n}$ is zero-mean Gaussian white noise vector; $\boldsymbol{\rho}$ is the amplitude matrix.

The parameters of Ship model uncertainty are chosen as follows.

$$\boldsymbol{\Delta}_f = \begin{bmatrix} 0.02\times 5.0242\times 10^4 u^2 + 0.01\times 5.0242\times 10^4 u^3 \\ 0.02\times 2.7299\times 10^5 v^2 + 0.01\times 2.7299\times 10^5 v^3 \\ 0.02\times 4.1894\times 10^8 r^2 + 0.01\times 4.1894\times 10^8 r^3 \end{bmatrix} \tag{43}$$

As automatic berthing systems use sliding mode controllers, the initial phase of the system is prone to a large range of control signals, which can have a significant impact on the ship. Therefore, a tracking differentiator [17] is added and a transition process is added to reduce the amount of overshoot in the system.

The parameters of the designed ESO are chosen as follows.

$\kappa_1 = 70, \kappa_2 = 800, \kappa_3 = 1000, \alpha_1 = 0.8, \beta_1 = 1.8;$

The parameters of finite-time controller parameters are selected as follows.

$a_1 = \mathrm{diag}([0.06, 0.05, 0.5]);$

$l_1 = \mathrm{diag}([2\times 10^{-3}, 10^{-2}, 6]);$

$r_1 = \mathrm{diag}([1,8,10]), r_2 = \mathrm{diag}([10,20,40]), l_2 = \mathrm{diag}([10^{-2}, 10^{-3}, 10^{-4}]);$

$l_3 = \mathrm{diag}([10^{-3}, 0.8\times 10^{-3}, 0.9\times 10^{-3}]);$

$a_2 = \mathrm{diag}([50,50,100]), \gamma_1 = 0.5;$

$r_3 = 10^{-3}\times \mathrm{diag}([2.5,3.5,5.5]), r_4 = 10^{-3}\times \mathrm{diag}([5.5,7.5,2.5]), \alpha_3 = 0.7, \alpha_4 = 0.7;$

$\alpha_2 = 0.6, \lambda_1 = \mathrm{diag}([0.5,0.5,0.5]), \lambda_2 = \mathrm{diag}([0.5,0.5,0.5]);$

$\varepsilon_1 = \mathrm{diag}([0.01, 0.080, 10]), \varepsilon_2 = \mathrm{diag}([100,100,100]);$

In this paper, the results are compared with the back-stepping berthing controller based on the uncertainty and disturbance estimator (UDE). Figure 2 to Figure 8 shows the simulation results of the external disturbance described by a value matrix $\boldsymbol{\rho} = diag\{8\times 10^6, 8\times 10^6, 8\times 10^6\}$

ISSN: 2472-3703 DOI: 10.6911/WSRJ.202205_8(5).0042

in the disturbance condition. The simulation results of the actual motion of the ship under the external disturbance and model uncertainty conditions are shown in Figure 3, and Figure 3 shows the trajectory of the ship during berthing. As can be seen from Figure 3, the ESO-based FTSM control method designed in this paper, the UDE-based control method and the UDE back-stepping based berthing control method designed in this paper can both reach the berthing point $(400\text{m}, 500\text{m}, 0^\circ)$ at a given initial position $(0\text{m}, 0\text{m}, 60^\circ)$ and remain stable to complete the berthing task.

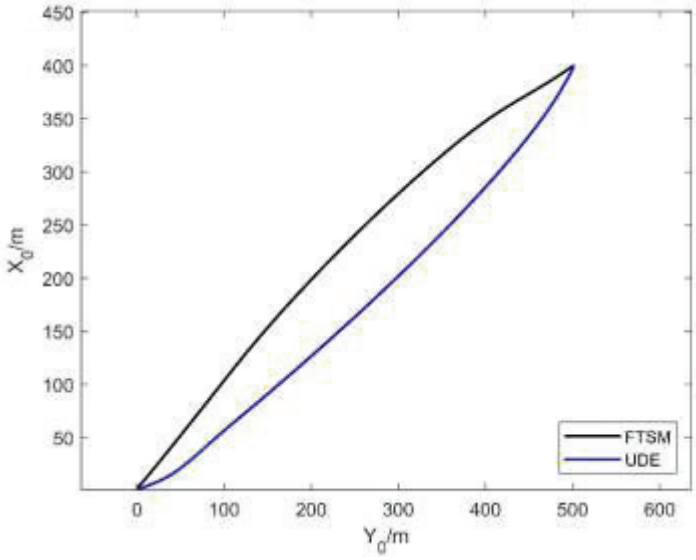


**Figure 2.** Actual ship berthing trajectory

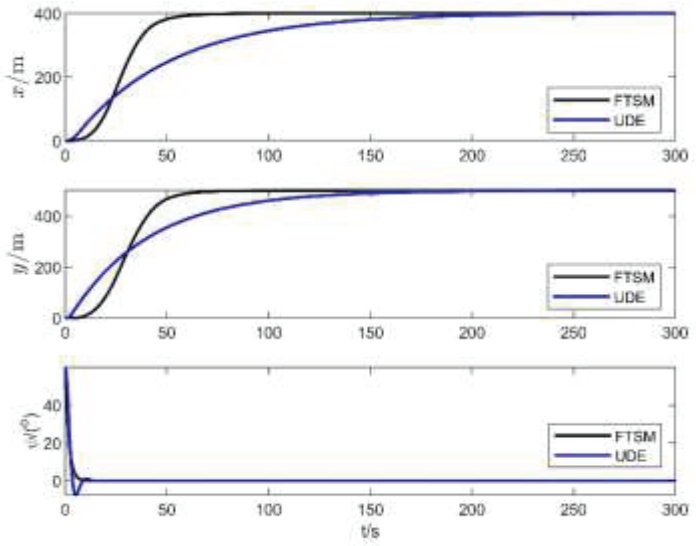


**Figure 3.** Position and heading angle of the ship

ISSN: 2472-3703 DOI: 10.6911/WSRJ.202205_8(5).0042

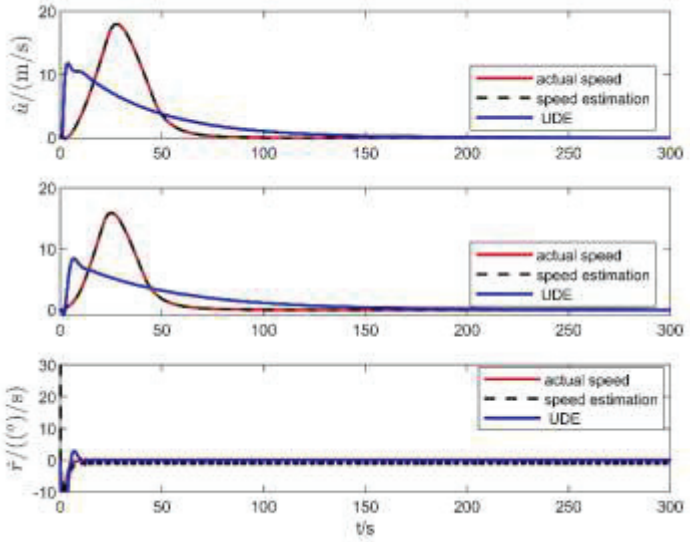


**Figure 4.** The estimation speed and real speed of the ship compared with UDE control method

Figure 3 shows that both this control method and the UDE back-stepping based berthing control method can get the ship to the desired position without overshoot and remain stable. The response time is fast.

According to Figure 4, the time response curves of the ship's longitudinal, transverse and bow motions velocities converge quickly to the zero range under external disturbances and model uncertainties. It can be further seen that the time response curves of the ship's longitudinal, transverse and bow-motion speeds under external disturbances and model uncertainty all converge to zero quickly; and the ESO-based FTSM control method converges significantly faster than the UDE control method, with a shorter berthing time, while the UDE-based control method reaches its maximum speed at 15s, but the speed convergence time is longer, resulting in a longer berthing time, so berthing time longer. Since, the ship speed state information is difficult to obtain accurately, the ship speed state information is estimated using ESO.

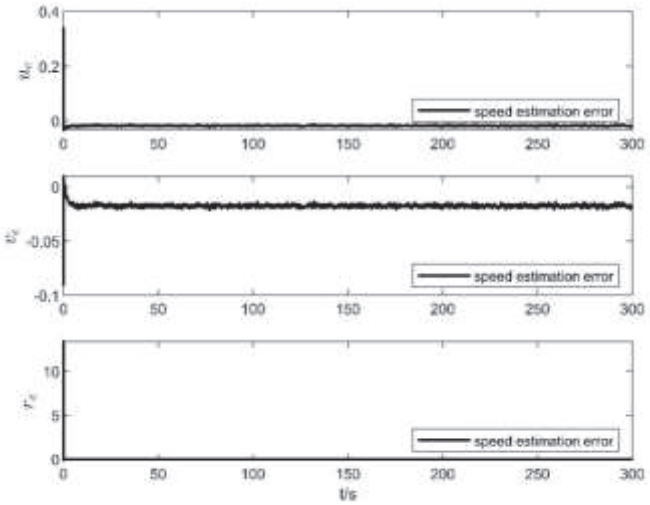


**Figure 5.** The speed estimation error of the ship

ISSN: 2472-3703 DOI: 10.6911/WSRJ.202205_8(5).0042

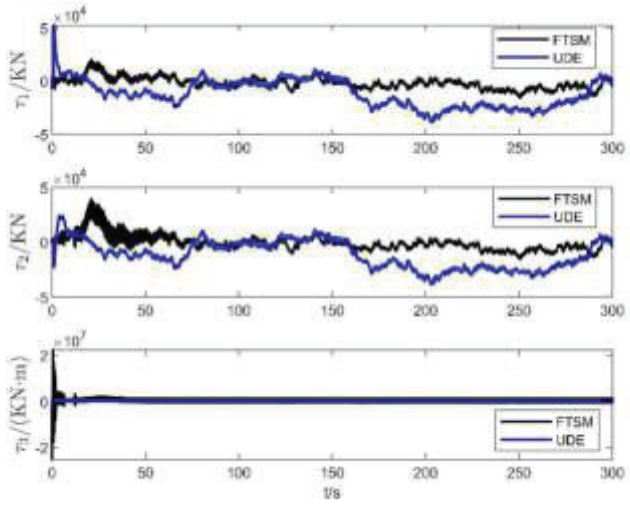


**Figure 6.** The control force and moment of the ship

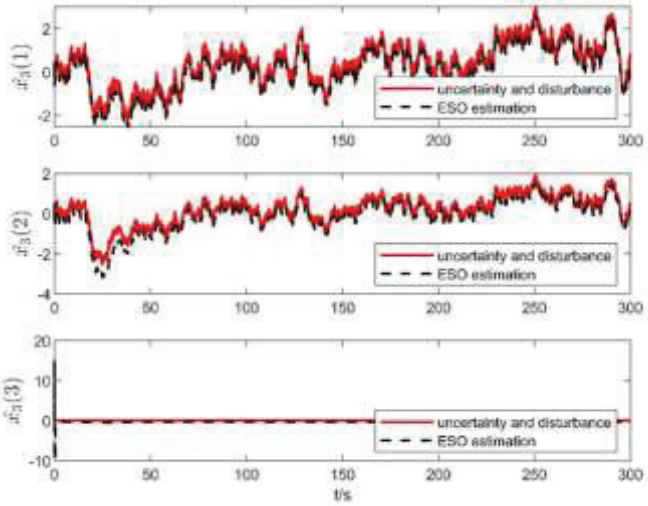


**Figure 7.** The estimation of external disturbance and model uncertainty state by ESO

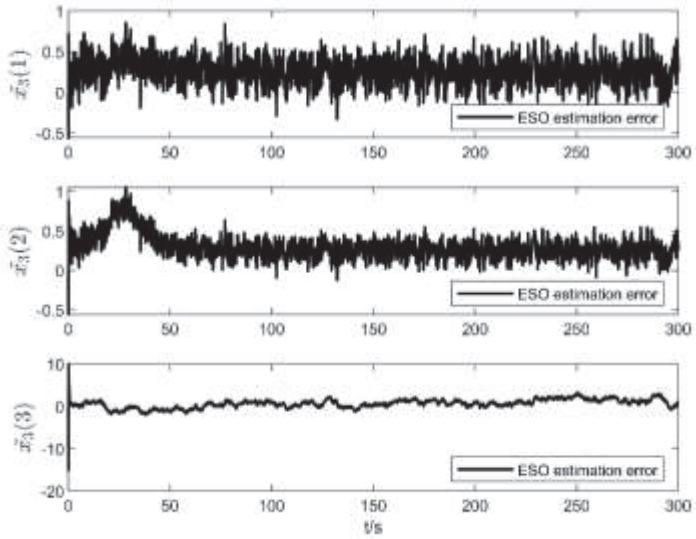


**Figure 8.** The estimation errors of external disturbance and model uncertainty state

ISSN: 2472-3703 DOI: 10.6911/WSRJ.202205_8(5).0042

Figure 5 shows that the estimation error value of the ship speed can converge quickly to near zero, and it can be seen from this figure that the estimation effect is better.

Figure 6 shows the output control forces and moments. Under the same disturbance conditions, the control forces and moments of the ESO-based FTSM control method are less variable, allowing the ship to reach the berthing position smoothly.

Figure 7 shows the estimated internal and external 'total disturbance' values of the ship, which compensate for the external disturbance and improve the control accuracy, by considering the complex disturbance as an expansion state.

Figure 8 shows the error of the complex perturbation state estimated by ESO versus the actual complex and the error converges.

Finally, the integral value of the product of time and absolute error is $I_{\mathrm{TAE}}=\int_0^t t|\tau|\mathrm{d}\tau$, which is used as the steady-state performance index to describe the two control methods, as shown in Table 1. $x_e$, $y_e$, and $\psi_e$ represent the ship position and bow tracking errors In Table 1. From Table 1, it can be seen that the value $I_{\mathrm{TAE}}$ of the ESO-based control method is significantly smaller than that of the UDE-based control method, which further demonstrates the better steady-state performance of the control method in this paper.

**Table 1.** Comparison of two control law performance

| Performance | $I_{\mathrm{TAE}}$ | | |
|---|---|---|---|
| **Errors** | $x_e$ | $y_e$ | $\psi_e$ |
| $\boldsymbol{\tau}_{\mathrm{UDE}}$ | $7.8\times10^5$ | $9.7\times10^5$ | 757.1 |
| $\boldsymbol{\tau}_{\mathrm{FTSM}}$ | $1.2\times10^4$ | $9.1\times10^4$ | 35.2 |

## 5. CONCLUSION

In this paper, during the process of automatic berthing, the problem of automatic berthing is solved under the circumstance of external disturbance, model uncertainty and inaccurate speed measurement. A finite-time fast terminal sliding mode of automatic berthing control controller is proposed through using ESO to estimate complex perturbations and speed. The experimental verification of a supply ship shows that the designed control method can estimate the complex perturbations and speed along with completing the automatic berthing task with good robustness with good control performance. However, in order to facilitate the design of the control method, the simple description of the external perturbation when the model is uncertain. The actuator saturation and ignoring the shore wall effect, these problems need to be studied later.

## REFERENCES

[1] C.S. Dai. Research on Adaptive Iterative Sliding Mode Control for Underactuated Ship Motion[D].Dalian,China:2017 ,Dalian Maritime University.

[2] R,X Bu, Z.J Liu, J.Q Hu. Berthing controller of underactuated ship with nonlinear sliding mode, Journal of Traffic and Transportation Engineering[J]. 2007(4): 24-29.

[3] Yao, Z. and G.E. Hearn, A multivariable neural controller for automatic ship berthing[J]. IEEE Control Systems, 1997. 17(4): p. 31-45.

ISSN: 2472-3703 DOI: 10.6911/WSRJ.202205_8(5).0042

[4] Piao, Guo, and Sun, Research into the Automatic Berthing of Underactuated Unmanned Ships under Wind Loads Based on Experiment and Numerical Analysis[J]. Journal of Marine Science and Engineering, 2019. 7(9): p. 300.

[5] Y.Liu, The Nonlinear Adaptive Control for Underactuated Surface Vessels [D].Dalian, China: 2017 ,Dalian Maritime University.

[6] Zhang, Q., et al., Adaptive neural network auto-berthing control of marine ships[J]. Ocean Engineering, 2019. 177(APR.1): p. 40-48.

[7] Z.J Piao. Research on automatic berthing control of unmanned surface vessel [D]. Dalian, China: 2017 ,Dalian Maritime University.

[8] McCue, L., Handbook of Marine Craft Hydrodynamics and Motion Control[J]. IEEE Control Systems, 2016. 36(1): p. 78-79.

[9] Borlaug, I.-L.G., K.Y. Pettersen, and J.T. Gravdahl, Comparison of two second-order sliding mode control algorithms for an articulated intervention AUV: Theory and experimental results[J]. Ocean Engineering, 2021. 222.

[10] Bhat, S.P. and D.S. Bernstein, Geometric homogeneity with applications to finite-time stability[J]. Mathematics of Control Signals & Systems, 2005. 17(2): p. 101-127.

[11] T.Q Wang. Research on Fixed-Time Trajectory Tracking Control Methods for Fully Actuated Vessels[D].Haerbing,China:2019, Harbin Engineering University.

[12] Peng, S. and Z. Lin, Finite-time command filtered backstepping control for a class of nonlinear systems[J]. Automatica, 2018.

[13] Wang, N. and F. Hao, Event-triggered sliding mode control with adaptive neural networks for uncertain nonlinear systems[J]. Neurocomputing, 2021. 436: p. 184-197.

[14] Shen, Q., et al., Integral-Type Sliding Mode Fault-Tolerant Control for Attitude Stabilization of Spacecraft[J]. IEEE Transactions on Control Systems Technology, 2015. 23(3): p. 1131-1138.

[15] Shen, Z., et al., Finite-time adaptive tracking control of marine vehicles with complex unknowns and input saturation[J]. Ocean Engineering, 2020. 198: p. 106980.

[16] Fossen, T.I. and J.P. Strand, Passive nonlinear observer design for ships using lyapunov methods: full-scale experiments with a supply vessel[J]. Automatica, 1999. 35(1).

[17] X.H Chen,X.B Niu. Ship dynamic positioning system control based on improved extended state observers [J]. Journal of Shanghai Maritime University, 2020. 41(04): 25-29+102.